Available online at www.sciencedirect.com
SCIENCE DIRECT®
Catalysis Today 98 (2004) 595–600
CATALYSIS TODAY
www.elsevier.com/locate/cattod

On the oxidative coupling of methane with carbon dioxide over CeO_2/ZnO nanocatalysts

Yongjun He, Bolun Yang*, Guangxu Cheng

Department of Chemical Engineering, Xi'an Jiaotong University, Xi'an 710049, PR China

Abstract

The nano-CeO_2/ZnO catalysts were prepared using a novel combination of homogeneous precipitation with micro-emulsion for oxidative coupling of methane with CO_2 as an oxidant. The prepared catalysts were compared with those prepared using the conventional impregnation. The catalysts prepared in two ways were characterized with FTIR, TEM, XRD and CO_2-TPD. The effects of the reaction temperature, the amount of ZnO doped in the catalysts and the average size were investigated. The experimental investigation demonstrated that methane conversion over the nano-CeO_2/ZnO catalysts prepared by the combined technique was higher than that obtained over catalysts prepared by the conventional impregnation. A better low-temperature activity has also been achieved over the nanocatalysts. There was no clear trend between the average size of nano-CeO_2/ZnO catalysts and their catalytic performance but methane conversion increased with increasing fractal dimension of nanocatalysts.

Keywords: Oxidative coupling; Methane; Carbon dioxide; CeO_2/ZnO; Catalyst preparation; Homogeneous precipitation; Micro-emulsion

1. Introduction

Ethylene is one of the most important basic chemicals in chemical industry. The present production of ethylene is principally via the pyrolysis of petroleum. With the gradual exhaustion of petroleum resources, alternative productions of ethylene are being explored worldwide. Oxidative coupling of methane with carbon dioxide provides us with a promising way of utilizing the relatively abundant natural gas resources and carbon dioxide, the largest man-made greenhouse gas [1,2]. However, because of the inert nature of molecules of methane and carbon dioxide, the preparation of a catalyst with sufficiently high activity remains as a big challenge to chemists all over the world [3,4].

Recently, nanocatalysts have attracted much attention [5–8]. The higher activity and better selectivity of nanocatalysts over traditional catalysts are attributed to their large specific surface area, high percentage of surface atoms and special crystal structures. The preparation methods, including homogeneous precipitation, micro-emulsion, gas evaporation, laser vaporization, ionized beam deposition and freezing drying, have a significant influence on the structure, size distribution and the morphology of the nanocatalysts, which in turn greatly affect the properties of the catalysts [9–13]. The method of combining the homogeneous precipitation with the micro-emulsion, using the water droplets of micro-emulsion as the nanoreactors for the homogeneous precipitation, may synthesize nanoparticles with a very narrow size distribution [14]. The average size of nanoparticles may be controlled to a certain extent by adjusting the reaction parameters, which make it possible to investigate the dependence of the performance of nanoparticles to their size.

In this work, the CeO_2/ZnO nanocatalysts were prepared by combining homogeneous precipitation with micro-emulsion. The catalysts were then applied for the oxidative coupling of methane with carbon dioxide as oxidant. A better low-temperature activity has been achieved this way.

* Corresponding author. Tel.: +86 29 82663189; fax: +86 29 82663547.
E-mail address: blunyang@mail.xjtu.edu.cn (B. Yang).

0920-5861/$ – see front matter © 2004 Elsevier B.V. All rights reserved.
doi:10.1016/j.cattod.2004.09.014

2. Experimental

2.1. Preparation of CeO_2/ZnO catalysts

2.1.1. The catalyst prepared by combining homogeneous precipitation with micro-emulsion

Cerium nitrate, zinc nitrate, zinc oxide, methyl oxalate, cetyl tri-methylamine bromide (CTAB), 1-hexyl alcohol, *n*-hexane and ethanol were commercially obtained (99.999% in purity; Xi'an Reagent Plant, China). To prepare the catalyst, CTAB and 1-hexyl alcohol were first added to 240 mL of *n*-hexane with agitation. Then 20 mL of aqueous solution, which contains cerium nitrate (0.12 mol/L), zinc nitrate (0.24 mol/L) and methyl oxalate (0.50 mol/L), was added into the solution of *n*-hexane with stirring until a transparent micro-emulsion was obtained. The micro-emulsion was heated to 318 K and was kept at this temperature for 4 h. The solvent was then recovered by distillation at the pressure of 75 mmHg. The residues were washed three times with ethanol and water, and dried under vacuum at 323 K for 2 h. Finally, the precursor was calcined at 973 K for 1 h. Following calcination, the cerium–zinc oxalate hydrates were converted into CeO_2/ZnO nanocatalysts.

By changing the calcination temperature and the molar ratio of methyl oxalate to cerium nitrate/zinc nitrate in the reaction mixture, the average size of CeO_2/ZnO nanocatalysts can be controlled.

2.1.2. The catalyst prepared by the conventional impregnation

Two grams of ZnO powder (40–60 mesh) was added into a 4-mL solution of cerium nitrate with a concentration of 0.35 mol/L under agitation. The mixture was then dried at 353 K for 5 h and calcined at 973 K in a muffle furnace for another 1 h. A light yellow CeO_2/ZnO catalyst was obtained this way.

2.2. Characterizations of catalyst

TEM characterization was conducted using a Hitachi H-600 transmission electron microscope. TGA/DTA analyses were carried out with a Dupont 2950 thermal analyzer in static air. Approximately 0.15 g of each sample was analyzed between 293 and 1273 K at 10 K/min using alumina crucibles. XRD patterns of the catalysts were obtained by a Rigaku D/MAX-3C X-ray diffraction system, using Co Kα radiation with 40 kV and 20 mA at a 0.2° scan rate (in 2θ). The FTIR spectra of the catalysts were obtained with a Nicolet Avatar 360 FTIR spectrometer in the 4000–400 cm^{-1} range. The average size of CeO_2/ZnO nanocatalysts was also measured by a Brookhaven BI-90 particle size analyzer.

In addition, CO_2-TPD analysis was carried out in a quartz tube with an inner diameter of 7 mm. The amount of catalyst loaded was 0.30 g. During the measurement, the catalyst was heated to 1173 K at 12 K/min under a 40 mL/min of He stream. The catalyst was then pre-activated at 1173 K for 40 min. After that, it was cooled to 303 K. A flowing CO_2 at a flow rate of 40 mL/min was switched into the quartz tube for 20 min. The catalyst was then swept with a 40 mL/min of He until there was no signal of CO_2 in the mass spectrum. The catalyst was cooled to room temperature before the desorption of CO_2. The CO_2-TPD analysis was finally carried out from room temperature to 1173 K at the heating rate of 12 K/min. The desorbed CO_2 was detected by an Omnistar mass spectrometer from Pfeiffer Vacuum.

2.3. Catalyst test

We evaluated the performance of the catalysts using the oxidative coupling of methane with carbon dioxide as an oxidant in a fixed-bed reactor with an inner diameter of 7 mm at atmospheric pressure. The amount of catalyst loaded was 0.30 g. Before reaction, the reactor was swept with a 45 mL/min of N_2 at the reaction temperature for 2 h. The feed gases, methane and carbon dioxide, at flow rates of 15 and 30 mL/min, respectively, were then introduced into the reactor. The feed and the effluent gases were analyzed by an online gas chromatograph (HP4890D).

3. Results and discussion

3.1. Characterization of CeO_2/ZnO catalysts

Fig. 1 presents a typical TEM image of CeO_2/ZnO nanocatalysts prepared by combining homogeneous precipitation with micro-emulsion (it will be referred as combining method in the following discussions). The CeO_2/ZnO nanocatalysts prepared this way had polyhedral morphology and good mono-dispersity. The average size of CeO_2/ZnO nanocatalysts was 32.5 nm, while the average size of the CeO_2/ZnO catalysts prepared by the conventional method was 347 nm (as shown in Fig. 2). However, the XRD patterns of these two kinds of catalysts were approximately the same (as shown in Fig. 3). The position and intensity of

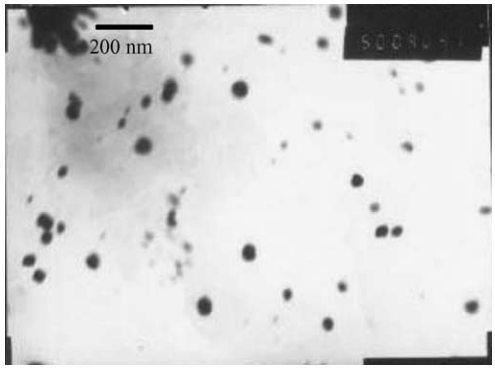

Fig. 1. TEM image of CeO_2/ZnO nanocatalysts prepared by the combining method.

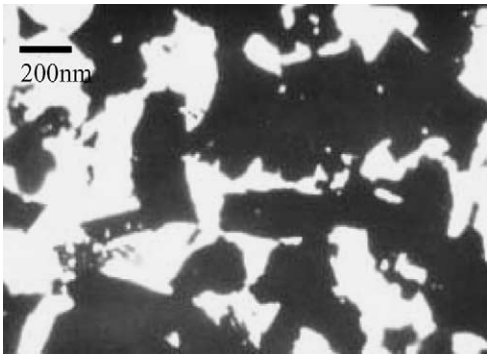

Fig. 2. TEM image of CeO_2/ZnO catalysts prepared by the conventional impregnation.

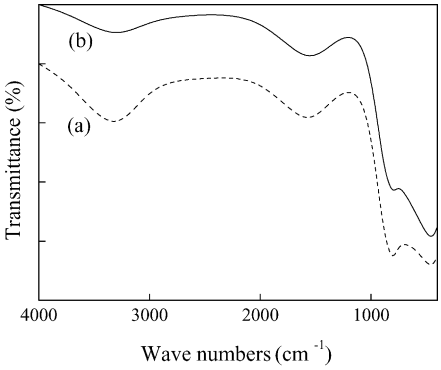

Fig. 4. FTIR spectra of CeO_2/ZnO catalysts: the catalyst prepared by the (a) combining method and (b) conventional method.

the diffraction peaks fitted well to JCPD card 05-0664 (ZnO) and 34-394 (CeO_2). There was no evidence of the generation of a new complex oxide.

The FTIR spectra of these two kinds of catalysts were also similar, except the nanocatalysts had a larger signal at wavenumbers from 3321.46 to 3531.68 cm^{-1}, which were attributed to the stretching modes of the absorbed water (see Fig. 4). Since the nanocatalysts had smaller size and higher specific surface area, their ability to adsorb water from the atmosphere was stronger.

Fig. 5 shows the CO_2-TPD results on the CeO_2/ZnO nanocatalysts prepared from the combining method, while Fig. 6 exhibits those obtained from the conventional impregnation. It can be seen that the area of the desorption peaks of CO_2 on nanocatalysts was much larger than that of the catalysts prepared by the conventional method. Obviously, the nanocatalysts had higher density of basic sites.

As shown in Figs. 5 and 6, both catalysts show two desorption peaks. The first presented at 338–383 K, which was attributed to the weak basic sites on the catalyst surface. The other was at 663–893 K, corresponding to the strong basic sites on the catalyst surface [15]. With the increasing doped ZnO, the intensity of the strong basic sites was reduced and that of the weak basic sites enhanced. This indicated that the addition of ZnO could modulate the intensity of the surface basicity of the catalysts.

3.2. Catalytic performance of CeO_2/ZnO catalysts

3.2.1. Effect of the reaction temperature

During the oxidative coupling reaction of methane with carbon dioxide as oxidant, the principal reactions are [2]:

$$CO_2 + 2CH_4 \rightarrow CO + C_2H_6 + H_2O$$

$$C_2H_6 \rightarrow C_2H_4 + H_2$$

The side reactions are:

$$CO_2 + CH_4 \rightarrow 2CO + 2H_2$$

$$CH_4 \rightarrow C + 2H_2$$

$$CO_2 + C \rightarrow 2CO$$

The results of the oxidative coupling of methane with carbon dioxide are shown in Fig. 7. The conversion of methane (X_{CH_4}) over the CeO_2/ZnO nanocatalysts was higher than that obtained over the conventional catalysts. In the case of the nanocatalysts, the oxidative coupling can take place at 923 K, which was ca. 100 K lower than the startup temperature over the conventional catalysts. The higher activity of the nanocatalysts could be attributed to their

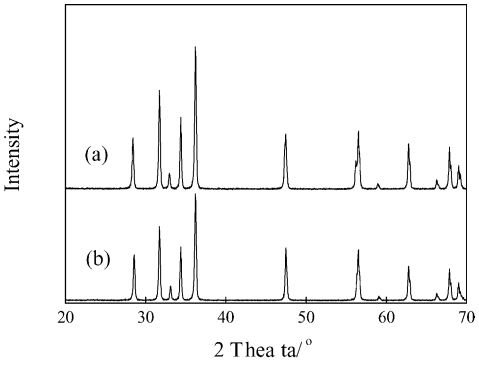

Fig. 3. XRD patterns of CeO_2/ZnO catalysts: the catalyst prepared by the (a) combining method and (b) conventional method.

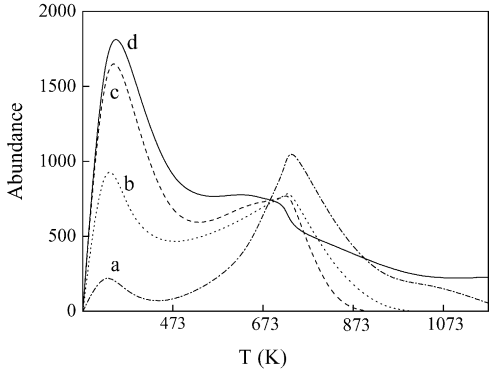

Fig. 5. CO_2-TPD profiles of the nanocatalysts prepared by the combining method (303 K): (a) CeO_2; (b) 80% CeO_2/ZnO; (c) 40% CeO_2/ZnO; (d) ZnO.

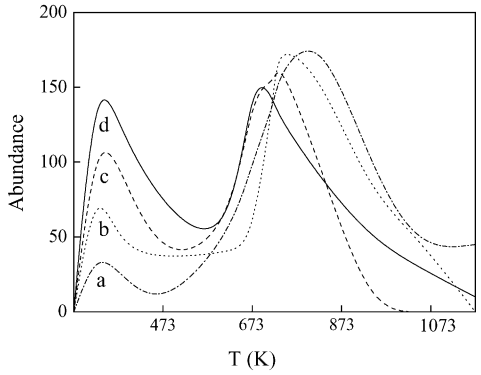

Fig. 6. CO_2-TPD profiles of the catalysts prepared by the conventional method (303 K): (a) CeO_2; (b) 80% CeO_2/ZnO; (c) 40% CeO_2/ZnO; (d) ZnO.

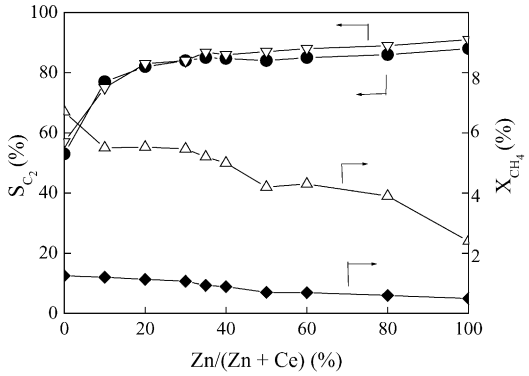

Fig. 8. Variation of catalytic performance with the amount of the doped ZnO at 1098 K: (△, ▽) nanocatalysts and (◆, ●) catalysts prepared by the conventional method.

smaller particle size, larger specific surface area and stronger intensity of surface basic sites [5,6].

The difference in the selectivity of C_2 hydrocarbon (S_{C_2}) between two catalysts was not significant, as shown in Fig. 7. It is thought that, since both catalysts had nearly the same crystal structure as shown in Fig. 2, the oxidative coupling reaction mechanism would be almost the same. And the nanocatalysts accelerated the rate of the principal reaction as well as that of the side reactions simultaneously.

The selectivity of C_2 hydrocarbon over both catalysts decreased quickly after 1073 K. It was found that more coke was formed on the surface of catalysts at higher temperatures.

3.2.2. *Effect of the amount of doped ZnO in the catalysts*

With the increase of the amount of the ZnO doped in the catalysts, the conversion of methane decreased and the selectivity of C_2 increased, as shown in Fig. 8. The adsorption of CO_2 on the surface of catalysts is the first step for the generation and circulation of active oxygen species O^-, which is the active species for the activation of methane [3,15]. From Figs. 5 and 6, the intensity of strong basic sites was reduced with the increase of the amount of the doped ZnO. Therefore the amount of CO_2 adsorbed on the surface of catalysts was also reduced, leading to the decrease of the O^- generated and thereby the conversion of methane. Meanwhile, the lower density of active oxygen species O^- also depressed the side reactions and increased the selectivity of C_2. When the content of ZnO in the nanocatalyst was 33%, the conversion of methane was 5.73% with the selectivity of C_2 of 83.6%. The yield of C_2 reached a maximum of 4.79%. The optimal yield of C_2 was lower than 1% over the conventional catalysts.

3.2.3. *Effect of the on-stream time*

With the elongation of the on-stream time, the amount of carbon deposition on the CeO_2/ZnO nanocatalysts increased much more quickly than that on the catalysts prepared by the conventional method, as shown in Fig. 9. This suggested that the nanocatalysts accelerated the side reaction of carbon deposition, as was assumed in Section 3.2.1.

The deposited carbon covered part of the active spots and baffled the diffusion of reactants, resulting in a more rapidly reduction in the activity of CeO_2/ZnO nanocatalysts than the catalysts prepared by the conventional method, as shown in Fig. 10.

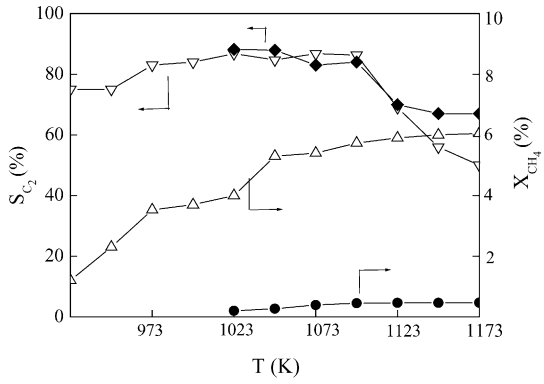

Fig. 7. Variation of the catalytic performance of 45% CeO_2/ZnO catalysts with reaction temperature: (△, ▽) nanocatalysts and (◆, ●) conventional catalysts.

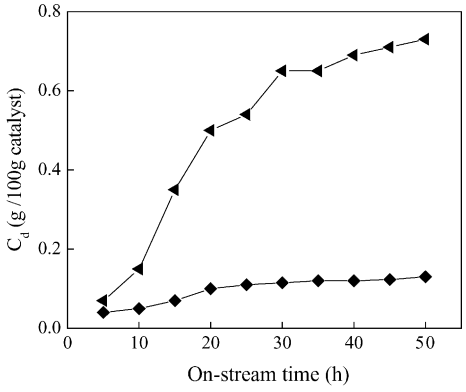

Fig. 9. Variation of the amount of carbon deposition on the 55% CeO_2/ZnO catalysts with the on-stream time at 1123 K: (▲) nanocatalysts and (◆) catalysts prepared by the conventional method.

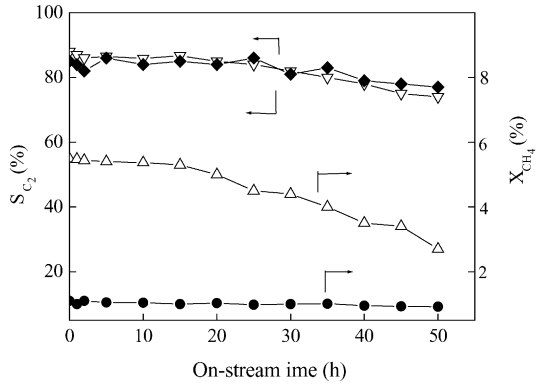

Fig. 10. Variation of catalytic performance of 55% CeO_2/ZnO catalysts with the on-stream time at 1123 K: (▽, △) nanocatalysts and (◆, ●) catalysts prepared by the conventional method.

Fig. 11 shows a TEM image of 55% CeO_2/ZnO nanocatalyst after reaction at 1123 K for 30 h. It can be seen that the average size of nanocatalysts increased from the initial 32.5 to 87 nm. The enlargement of the average size of nanocatalysts was possibly another reason for the decrease of the catalytic activity.

3.2.4. Effect for the average size of nanocatalysts

By changing the preparation conditions, the CeO_2/ZnO nanocatalysts with different sizes were prepared. The effect of the average size on the performance of the nanocatalysts is shown in Fig. 12. From Fig. 12, it was shown that the effect of the catalyst size was not significant.

3.3. Fractal feature of CeO_2/ZnO nanocatalysts

Pfeifer and Avnir successfully applied the fractal theory for description of heterogeneous catalysts [16]. Many subsequent experiments have proved that the fractal dimension (D_f) of catalysts has some connection to their catalytic performance and can serve as a supplementary parameter to express the surface characteristics of catalysts [17–20].

In this work, the box dimension model was used to calculate the fractal dimension of nanocatalysts [20]. Fig. 13

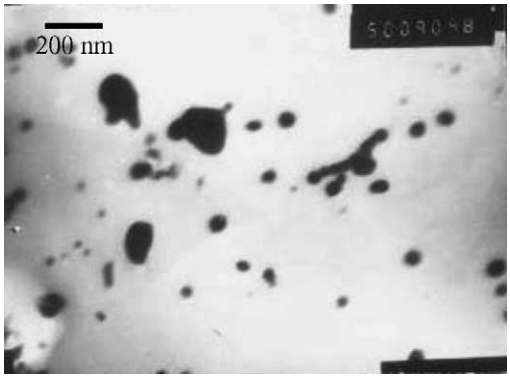

Fig. 11. TEM image of 55% CeO_2/ZnO nanocatalyst after reaction at 1123 K for 30 h.

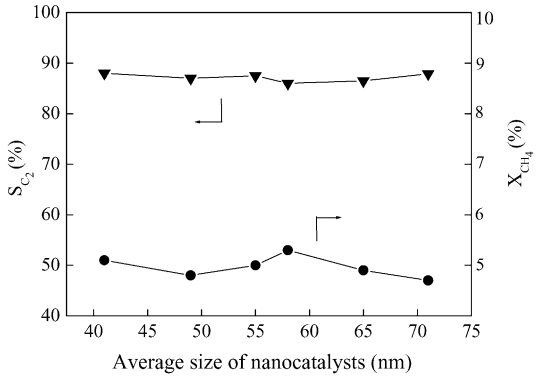

Fig. 12. Variation of the catalytic performance at 1148 K with the average size of 40% CeO_2/ZnO nanocatalysts prepared by the combining method.

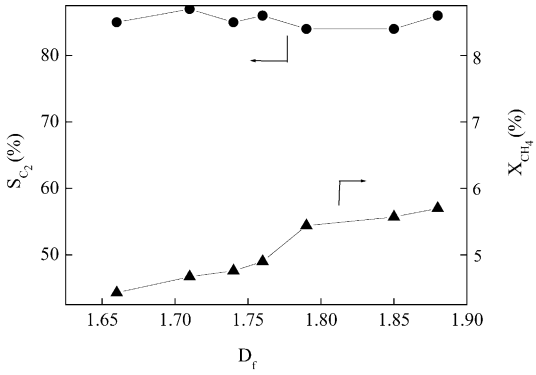

Fig. 13. Variation of methane conversion with the fractal dimension of 30% CeO_2/ZnO nanocatalysts.

shows the variation of the conversion of methane and the selectivity of C_2 with the fractal dimension of nanocatalysts at 1148 K. As shown in this figure, the conversion of methane increased with the increasing fractal dimension of nanocatalysts. However, the influence on the C_2 selectivity was not remarkable. It is well known that the catalytic performance of heterogeneous catalysts was mainly determined by their geometric and electronic features. The fractal dimension is the measurement of the geometric features of the catalyst surface [16]. Larger fractal dimension indicates more defect structures on the catalyst surface, which means a higher activity of the catalysts with higher conversion of methane. The electronic features of catalysts basically affected the selectivity of C_2, while the fractal dimension could not reflect such electronic features. There was no direct connection of the selectivity of C_2 to the fractal dimension of catalysts.

4. Conclusions

CeO_2/ZnO nanocatalysts were prepared from a novel combination of homogeneous precipitation with micro-emulsion. The catalytic performance of the nanocatalysts on the oxidative coupling of methane with carbon dioxide as the

oxidant was investigated and compared with that of the catalysts prepared by the conventional impregnation. Experimental results showed that the conversion of methane over the CeO_2/ZnO nanocatalysts was higher than that obtained from the catalysts prepared conventionally. A better low-temperature activity has also been achieved with a higher yield of C_2 hydrocarbons. With an increase in the amount of the doped ZnO in the nanocatalysts, the conversion of methane decreased while the selectivity of C_2 increased. There was no correlation between the conversion of methane and the average size of the nanoparticles, but the conversion of methane improved with increasing fractal dimensions of the nanocatalysts.

References

[1] Y. Wang, Y. Takahashi, Y. Ohtsuka, Appl. Catal. A: Gen. 72 (1998) L203.
[2] K. Asami, T. Fujita, K. Kusakabe, Appl. Catal. A: Gen. 126 (1995) 245.
[3] C. Chen, Y. Xu, G. Li, J. Catal. Lett. 42 (1996) 149.
[4] A. Hagfeld, M. Gratzel, Chem. Rev. 95 (1995) 49.
[5] Y.K. Won, H. Hiroki, K. Masahiro, Appl. Catal. A: Gen. 169 (1998) 157.
[6] H. Wang, J. Wang, W.D. Xiao, Powder Technol. 111 (2000) 175.
[7] T.R. Thurston, J.P. Wilcoxon, J. Phys. Chem. B 103 (1999) 11.
[8] J.D. Aiken, R.G. Finke, J. Mol. Catal. A: Chem. 145 (1999) 1.
[9] S.W. Guo, L. Konopny, R. Popovitz-Biro, Adv. Mater. 12 (2000) 302.
[10] W.H. Wang, D.W. He, D.Q. Zhao, Appl. Phys. Lett. 75 (1999) 2770.
[11] J.C. Hulteen, D.A. Treichel, M.T. Smith, J. Phys. Chem. B 103 (1999) 3854.
[12] X.G. Peng, L. Manna, W.D. Yang, Nature 404 (2000) 59.
[13] X. Mo, C. Wang, L. Hao, Mater. Res. Bull. 36 (2001) 1925.
[14] Y.J. He, B.L. Yang, G.X. Cheng, Mater. Lett. 57 (2003) 1880.
[15] C. Chen, Y. Xu, G.G.X. Guo, Catal. Lett. 42 (1996) 149.
[16] P. Pfeifer, D. Avnir, J. Chem. Phys. 79 (1983) 3558.
[17] R. Larraz, J. Chem. Eng. 86 (2002) 309.
[18] M. Coppens, Colloid. Surf. A: Physicochem. Eng. Aspects 187–188 (2001) 257.
[19] M.O. Coppens, Catal. Today 53 (1999) 225.
[20] C. Huo, X. Ren, Y. Zong, Y. Yang, Petrochem. Technol. 28 (1999) 820.